

2

AD-A272 972

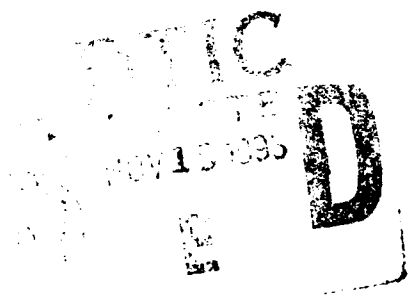
NASA Technical Memorandum 109021
ICASE Report No. 93-60

ICASE



NUMERICAL SIMULATION OF THREE-DIMENSIONAL SELF-GRAVITATING FLOW

John V. Shebalin



August 1993

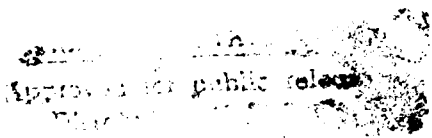
Institute for Computer Applications in Science and Engineering
NASA Langley Research Center
Hampton, Virginia 23681-0001

Operated by the Universities Space Research Association

93-28041



National Aeronautics and
Space Administration
Langley Research Center
Hampton, Virginia 23681-0001



93 11 15 070

ICASE Fluid Mechanics

Due to increasing research being conducted at ICASE in the field of fluid mechanics, future ICASE reports in this area of research will be printed with a green cover. Applied and numerical mathematics reports will have the familiar blue cover, while computer science reports will have yellow covers. In all other aspects the reports will remain the same; in particular, they will continue to be submitted to the appropriate journals or conferences for formal publication.

DATE QUALITY INSPECTED 3

Accession For	
NTIS CRA&I	<input checked="" type="checkbox"/>
DTIC TAB	<input type="checkbox"/>
Unannounced	<input type="checkbox"/>
Justification	
By _____	
Distribution/	
Availability Codes	
Dist	Avail and/or Special
A-1	

Numerical Simulation of Three-Dimensional Self-Gravitating Flow

John V. Shebalin*

National Aeronautics and Space Administration

Langley Research Center

Hampton, Virginia 23681, USA

The three-dimensional flow of a self-gravitating fluid is numerically simulated using a Fourier pseudospectral method with a logarithmic variable formulation. Two cases with zero total angular momentum are studied in detail, a 32^3 simulation (Run A) and a 64^3 simulation (Run B). Other than the grid size, the primary differences between the two cases are that Run A modelled atomic hydrogen and had considerably more compressible motion initially than Run B, which modelled molecular hydrogen. The numerical results indicate that gravitational collapse can proceed in a variety of ways. In the Run A, collapse led to an elongated tube-like structure, while in the Run B, collapse led to a flatter, disk-like structure.

*Research supported by the National Aeronautics and Space Administration. This work was done while the author was in residence as a Visiting Scientist at the Institute for Computer Applications in Science and Engineering (ICASE), NASA Langley Research Center, Hampton, VA 23681.

1 Introduction

In recent years, Fourier methods have been used to simulate collapse of a gas due to a newtonian gravitational self-interaction, both in one-dimension (1D) and in two-dimensions (2D). In the 1D case [1], the flow was assumed to be isentropic, 64 grid points were used, and it was found necessary to modify the values of density at each time-step by adding a spatial constant so as to ensure sufficient positive-definiteness of the density at all grid points. In the 2D case [2], the flow was again assumed isentropic, the maximum grid size was 256^2 , the density was again 'modified' to ensure numerical stability, and, in addition, the flow was initially turbulent (with the notable result of hindering collapse).

Here, this work is extended in four ways. First the full polytropic gas-dynamic equations are solved with no isentropic approximation. (Collapse is assumed to take place on length and time scales such that no overall cosmological expansion need be imposed on the dynamics.) Second, simulations are performed on three-dimensional grids (32^3 and 64^3). Third, the governing equations are written so that the logarithms of the density and temperature are solved for, rather than the density and temperature directly. This allows explicitly for the preservation of positive-definiteness of density, temperature, and pressure, since these are arrived at by exponentiation. Fourth, bulk viscosity is utilized to model more accurately the properties of molecular hydrogen.

These extensions allow for more realistic simulations of the self-gravitational collapse of clouds of either atomic (H) or molecular (H_2) hydrogen, at least up to the point where density gradients are so steep that the computer code loses accuracy. In particular, two cases with zero total angular momentum are studied in detail, one on a 32^3 grid (Run A: H) and the other on a 64^3 grid (Run B: H_2). The primary difference between the two cases (other than grid size and chemical constituents) lies in the ratio of compressible kinetic energy to total kinetic energy. Run A had an initial ratio of 0.5, while Run B had an initial ratio of 0.1. Collapse from a constant density initial state is clearly different for the two cases: in Run A, the collapse is to a tube-like structure, while in Run B, it is to a flat, disk-like structure (a Zeldovich 'pancake' [3]).

Following brief descriptions of the governing equations and numerical method, numerical results will be discussed. Flow parameters will be defined, as well as measures of anisotropy which are useful for quantitatively describing self-gravitational collapse. Finally, a summary and conclusion will be presented.

2 Physics & Numerics

Placing $\rho = e^\lambda$ and $T = e^\sigma$ into the standard polytropic gas equations yields the basic non-dimensional equations in a logarithmic formulation [4]:

$$\frac{\partial \lambda}{\partial t} + \mathbf{u} \cdot \nabla \lambda = -\nabla \cdot \mathbf{u} \quad (1)$$

$$\begin{aligned} \frac{\partial \mathbf{u}}{\partial t} + \mathbf{u} \cdot \nabla \mathbf{u} = & -\frac{1}{\gamma} e^\sigma \nabla(\lambda + \sigma) - \nabla \Phi \\ & + \frac{\mu}{e^\lambda} \nabla \cdot \left[\nabla \mathbf{u} + \left(\frac{1}{3} + \beta \right) \mathbf{I} \nabla \cdot \mathbf{u} \right] \end{aligned} \quad (2)$$

$$\begin{aligned} \frac{\partial \sigma}{\partial t} + \mathbf{u} \cdot \nabla \sigma = & -(\gamma - 1) \nabla \cdot \mathbf{u} + \frac{\kappa}{e^\lambda} [\nabla^2 \sigma + (\nabla \sigma)^2] \\ & + \frac{\gamma(\gamma - 1)\mu}{e^{(\lambda + \sigma)}} \left[\frac{1}{2} \tau_{ij} \tau_{ij} + \beta (\nabla \cdot \mathbf{u})^2 \right] \end{aligned} \quad (3)$$

Here, $\tau_{ij} = \partial_i u_j + \partial_j u_i - 2/3 \delta_{ij} \nabla \cdot \mathbf{u}$ and $\mathbf{I} = [\delta_{ij}]$ is the unit dyadic. In (2), Φ is the newtonian gravitational potential which satisfies $\nabla^2 \Phi = k_J^2 \rho$, where k_J is the Jeans wavenumber [5]; for Run A, $k_J = \sqrt{2}$ and for Run B, $k_J = 1.5$. The adiabatic index γ is constant, and since the gas is either H or H_2 , $\gamma = 5/3$ for Run A and $\gamma = 7/5$ for Run B. The dimensionless shear viscosity μ and thermal conductivity κ are also constant; the Prandtl number, $Pr = \gamma\mu/\kappa$, has a value of ~ 1 , which will determine κ : $\kappa = \gamma\mu$ ($\mu = 0.02$ for Run A and $\mu = 0.005$ for Run B). The ratio of bulk to shear viscosity, $\beta = \mu_B/\mu$, will also be constant: $\beta = 1$ for Run A (to represent a small admixture of H_2 with primarily H) and $\beta = 32$ for Run B (only H_2) [6].

Details of the numerical method used here have been given previously [4, 7]. The only modification lies in the addition of the self-gravitation term $-\nabla \Phi$ in (2). Using $\nabla^2 \Phi = k_J^2 \rho$ and Fourier transformation gives $-\nabla \Phi \rightarrow ik_J^2 \mathbf{k} k^{-2} \rho(\mathbf{k})$, which is very straightforward to implement when (1)–(3) are written in terms of Fourier coefficients (as is done in the method utilized here). We now proceed on to the results of the simulations.

3 Results

Run A used a 32^3 spatial grid and ran a total of 15300 time-steps (Δt 's), with 2 cpu-sec/ Δt on a Cray YMP.

Run B used a 64^3 spatial grid and ran a total of 49800 Δt 's, with 13 cpu-sec/ Δt , also on a Cray YMP.

Run A was terminated at simulation time $t = 6.57$ when the dissipation wave number k_D (as defined in [4]) had increased so as to equal the maximum wave number $k_{max} = 16$. Similarly, Run B was terminated at simulation time $t = 5.01$ when the dissipation wave number k_D had increased so as to equal its maximum wave number $k_{max} = 32$. The microscale Reynolds number R_λ (also defined in [4]) ranged between 17 and 32 for Run A, and between 90 and 170 for Run B.

In the following, $\langle Q \rangle$ will denote the volume average (or average value per grid point) of any quantity Q . Thus, the various energies associated with the collapsing clouds of gas are the kinetic energy $E_K = \langle \rho u^2 / 2 \rangle$, the internal energy $E_I = \langle \rho T / [\gamma(\gamma - 1)] \rangle$, the gravitational energy $E_G = \langle \rho \Phi / 2 \rangle$, and the total energy $E = E_K + E_I + E_G$. The time evolution of these energies is shown in Figure 1 for Runs A and B.

As is evident in Figure 1, collapse did not begin immediately, but rather after the initial turbulent motion had decayed to a lower level, in accord with previous results [2]. (The initial turbulent velocity spectra was $|\mathbf{u}(\mathbf{k})|^2 \sim k^4 \exp -2k^2/k_o^2$, with $k_o = 3$ for Run A and $k_o = 4$ for Run B.) However, once collapse had progressed sufficiently, both the mean-squared dilatation $\Psi \equiv \frac{1}{2} \langle (\nabla \cdot \mathbf{u})^2 \rangle$ and the mean-squared vorticity (the enstrophy) $\Omega \equiv \frac{1}{2} \langle (\nabla \times \mathbf{u})^2 \rangle$ began to increase. This is shown in Figure 2, where it is clear that Run A had more compressible velocity initially than Run B did. [The compressible part of the velocity is $\mathbf{u}_c(\mathbf{k}) \equiv k^{-2} \mathbf{k} \mathbf{k} \cdot \mathbf{u}(\mathbf{k})$.] Note that both Ψ and Ω begin to increase near the end of the runs.

The relative amount of compressible velocity in a flow is quantified by the ratio $\chi = \langle u_c^2 \rangle / \langle u^2 \rangle$, whose importance was first recognized by Passot and Pouquet [8]. The time evolution of χ for Runs A and B is shown in Figure 3. For Run A, $\chi \simeq 0.25$ before collapse initiates, while for Run B, $\chi \simeq 0.02$ during the equivalent time period. Although there are many differences between Runs A and B, the qualitatively different behavior of χ prior to collapse may be related to the qualitatively different dynamical behavior of the gas in Runs A and B during the collapse itself.

The results of gravitational collapse in Runs A and B are seen in Figures 4 and 5. These figures represent the densities of the respective clouds of gas at the end of each run and are drawn by finding the point of maximum density in either run, extracting values of density on the three orthogonal planes ($x - y$, $y - z$, and $z - x$) which contain this point, and then shifting the points on these periodic planes so that the maximum density lies in their centers. In Figure 4 it is clear that the gas has collapsed to a tube-like structure: in Figure 5 it is clear that the gas has collapsed to a much flatter, somewhat irregular, disk-like structure.

In order to get a better picture of how these structures developed, it is useful to define the following measures of anisotropy M_j ($j = x, y, z$) [9]:

$$M_j = \frac{3 \langle (\partial_j \rho)^2 \rangle}{2 \langle (\nabla \rho)^2 \rangle} - \frac{1}{2} \quad (4)$$

The time evolution of the M_j for Runs A and B are shown in Figure 6. Note that the differences in the final states of Runs A and B, as shown in Figures 4 and 5, grew directly from their initial states, rather than going through a qualitatively different intermediate stage.

4 Summary & Conclusion

In this work a three-dimensional pseudospectral computer code was used to simulate the initial stages of the gravitational collapse of clouds of either atomic or molecular hydrogen. The full polytropic gasdynamic equations were solved, with the primary dynamical variables being $\ln \rho$, $\ln T$, and \mathbf{u} . In addition to shear viscosity, bulk viscosity was also utilized to more exactly model the properties of molecular hydrogen.

Two runs were examined in detail, Run A (on a 32^3 grid) and Run B (on a 64^3 grid). As the figures show, the nature of the collapse was different for each run: in Run A, the collapse proceeded to a quasi-1D structure, while in Run B, the collapse proceeded to a quasi-2D structure. One primary difference between the runs lay in the relative amount of compressible turbulent kinetic energy prior to collapse. This suggests that turbulent density fluctuations may have an important role to play during gravitational collapse.

There is a large amount left unexplored in all of this, with respect to variation in initial conditions, transport properties, and grid size, or with respect to the effects of magnetic fields or radiation, for example. The sheer length of a single, moderately resolved simulation ($64^3 \rightarrow \sim 200$ Cray YMP cpu-hours) precludes any quick but thorough investigation of ‘parameter space.’ Instead, it is clear that only a slow and patient effort (along with exponential increases in computer power) will yield the results and insight which are sought.

References

- [1] G. Alecian & J. Léorat, 'Homogeneous self-gravitating flows,' *Astron. Astrophys.*, **196**, 1-16 (1988).
- [2] J. Léorat, T. Passot, & A. Pouquet, 'Influence of supersonic turbulence on self-gravitating flows,' *Mon. Not. R. Astr. Soc.*, **243**, 283-311 (1990).
- [3] Ya. B. Zeldovich, 'Gravitational Instability: An Approximate Theory for Large Density Perturbations,' *Astron. Astrophys.*, **5**, 84-89 (1970).
- [4] J. V. Shebalin, 'Pseudospectral simulation of compressible turbulence using logarithmic variables,' *Proceedings of the 11th AIAA Computational Fluid Dynamics Conference*, 841-851, Orlando, FL (1993).
- [5] J. Binney & S. Tremaine, *Galactic Dynamics*, p. 291, Princeton U. P., Princeton, NJ (1972).
- [6] P. A. Thompson, *Compressible-Fluid Dynamics*, p. 30, McGraw-Hill, New York (1972).
- [7] J. V. Shebalin and D. Montgomery, 'Turbulent magnetohydrodynamic density fluctuations,' *J. Plasma Phys.*, **39**, 339-367 (1988).
- [8] T. Passot and A. Pouquet, 'Numerical simulation of compressible homogeneous flows in the turbulent regime,' *J. Fluid Mech.*, **181**, 441-446, 1987.
- [9] C. G. Speziale, S. Sarkar, & T. B. Gatski, 'Modelling the pressure-strain correlation of turbulence: an invariant dynamical systems approach,' *J. Fluid Mech.*, **227**, 245-272 (1991).

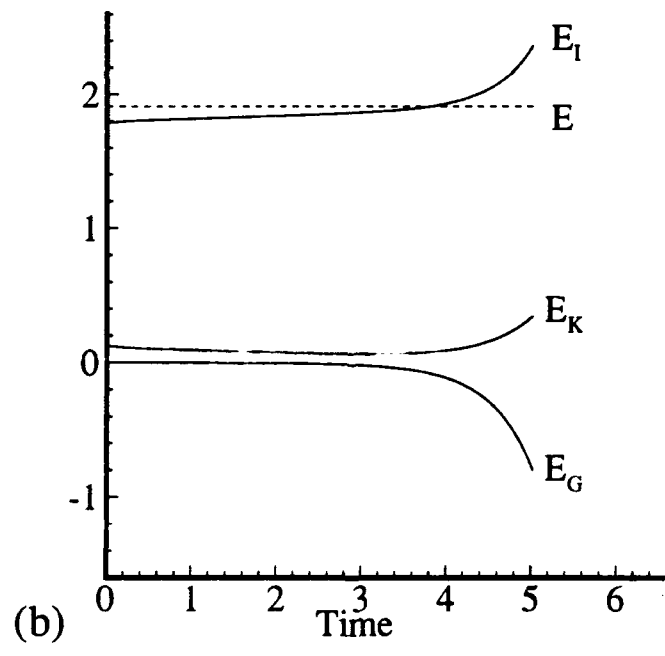
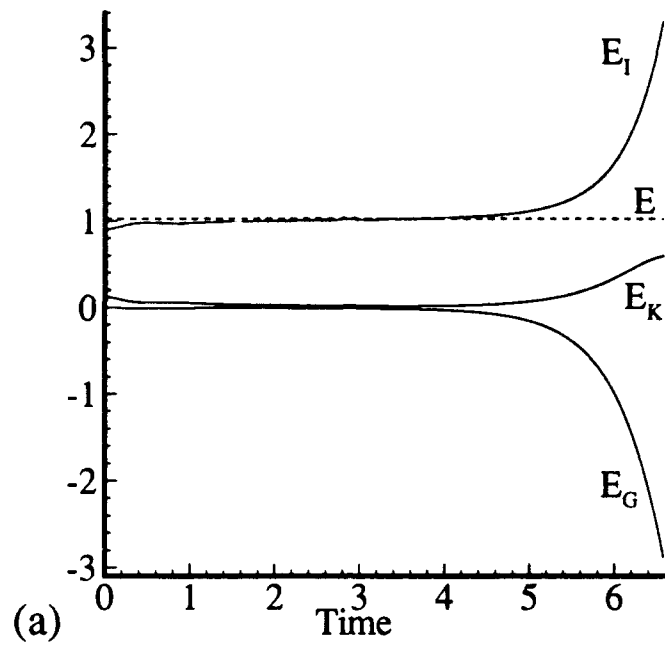


Figure 1. Energies vs time for (a) Run A and (b) Run B.

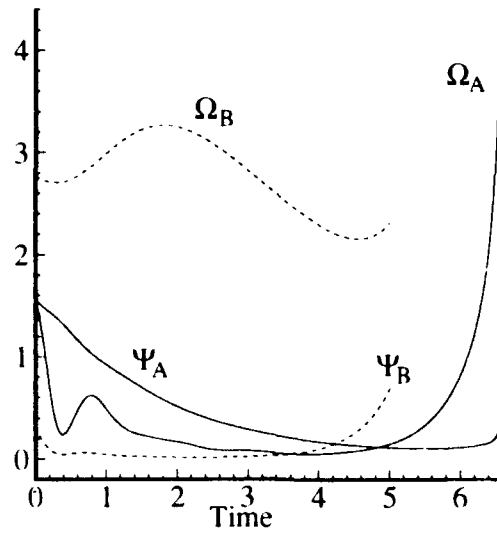


Figure 2. Enstrophy Ω and mean-squared dilatation Ψ for Runs A and B.

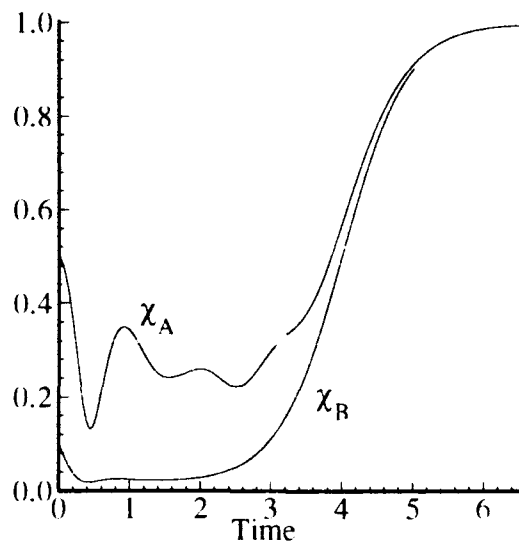


Figure 3. Compressibility ratio χ for Runs A and B.

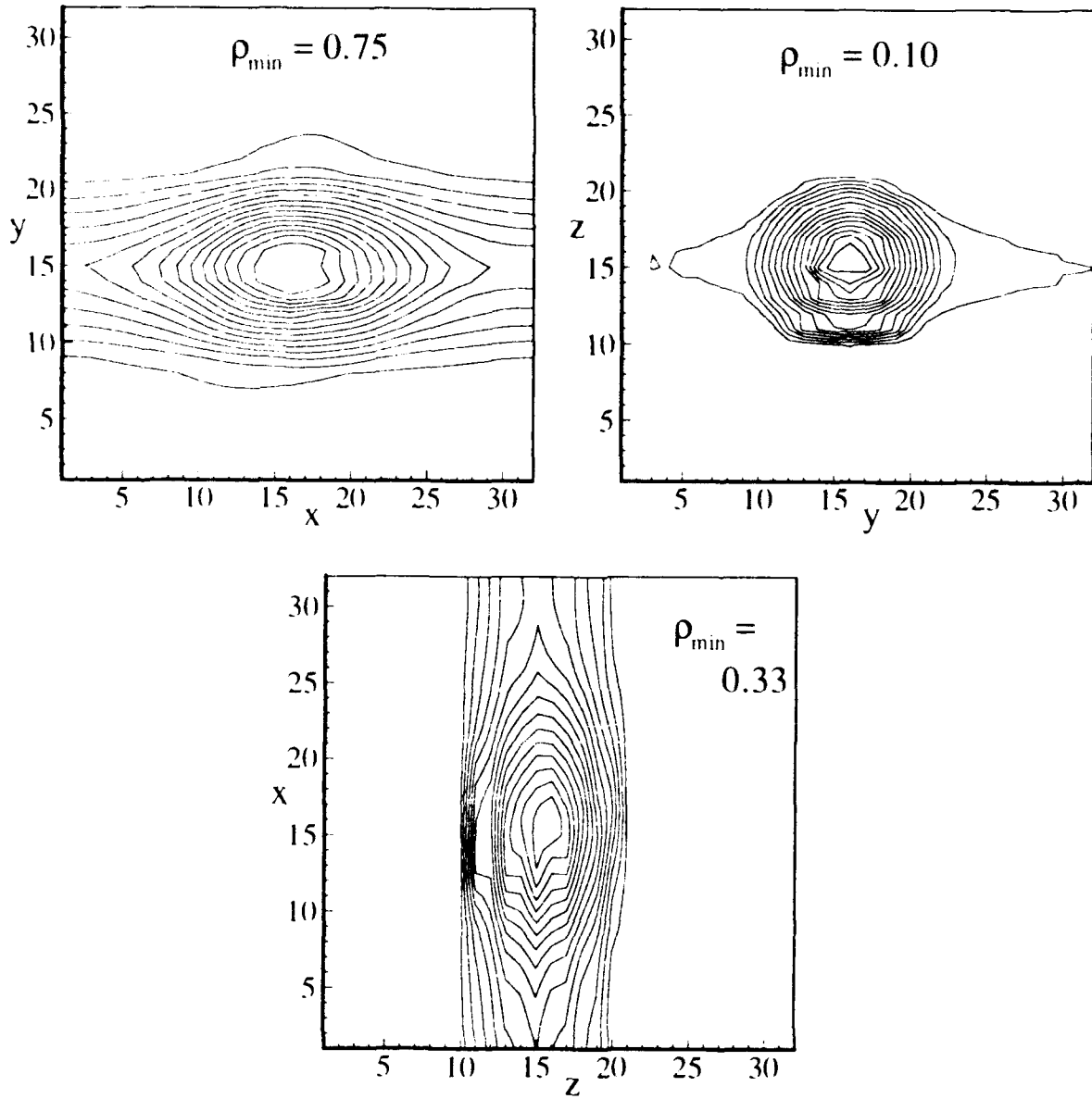


Figure 4. Density contours in orthogonal planes intersecting the point of maximum density ($\rho_{\max} = 22.2$) at $t=6.57$ for Run A.

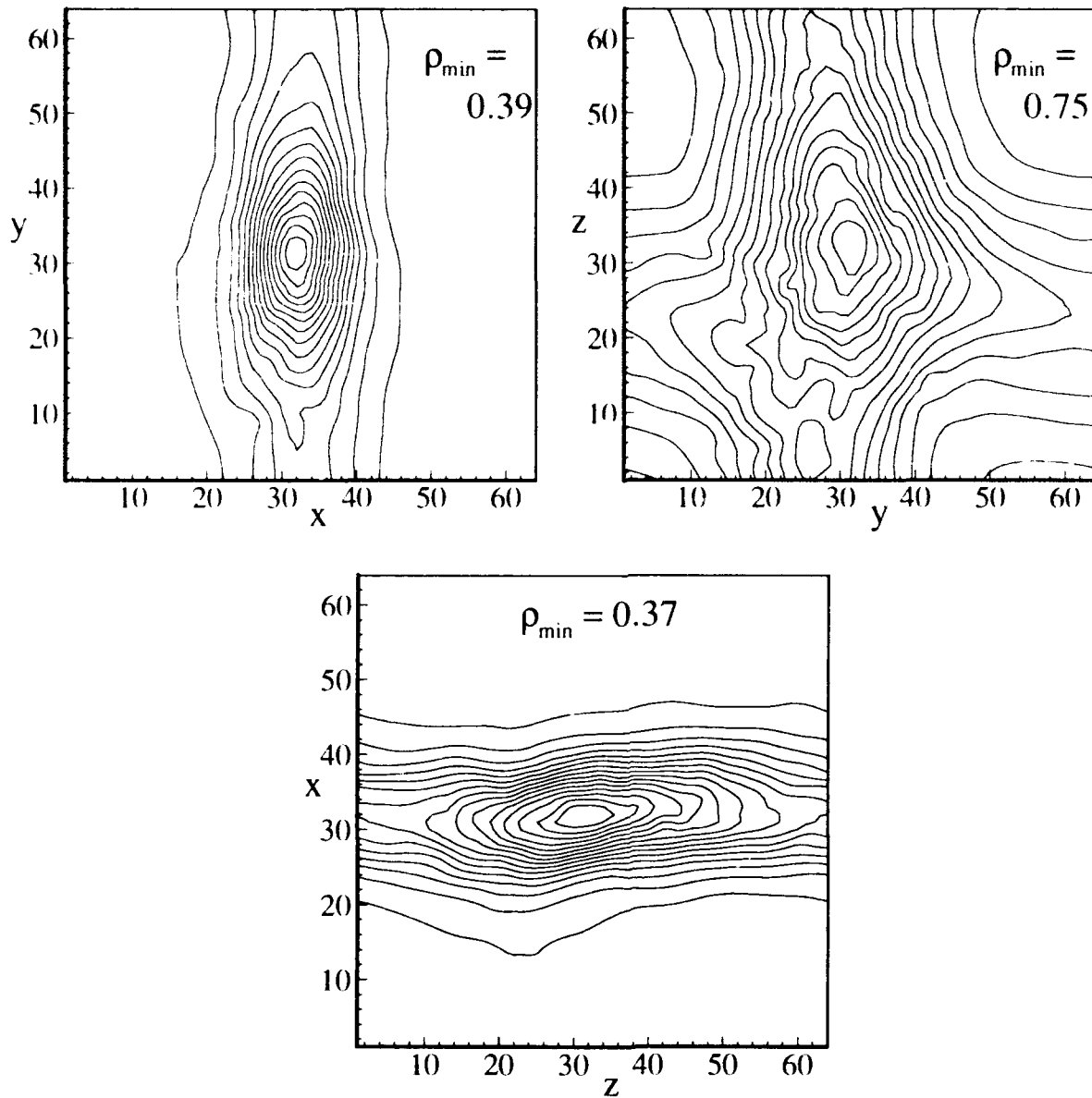


Figure 5. Density contours in orthogonal planes intersecting the point of maximum density ($\rho_{\max} = 0.79$) at $t=5.01$ for Run B.

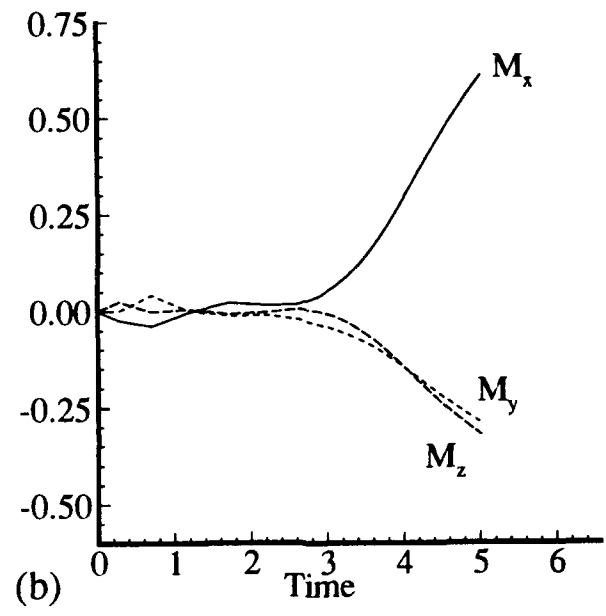
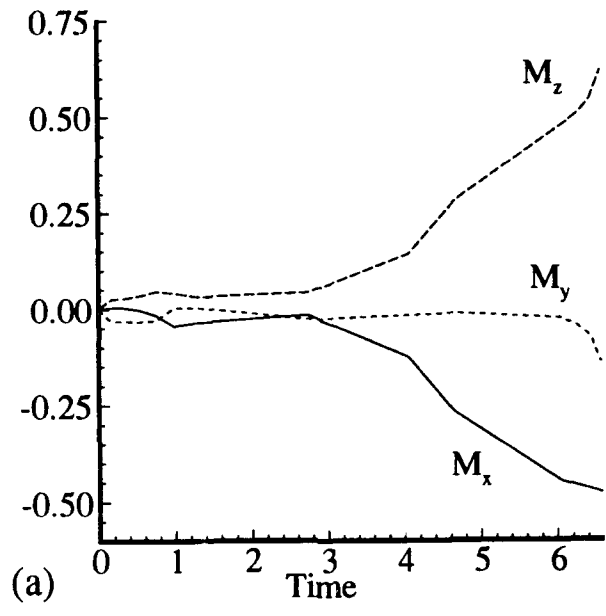


Figure 6. Measures of anisotropy for (a) Run A and (b) Run B.

